J Acupunct Meridian Stud 2012;5(3):126–135

Available online at www.sciencedirect.com

Journal of Acupuncture and Meridian Studies

journal homepage: www.jams-kpi.com

RESEARCH ARTICLE

Regenerative Effects of Moxibustion on Skeletal Muscle in Collagen-Induced Arthritic Mice☆

Min-Jung Kim, Uk Namgung, Kwon-Eui Hong*

Department of Oriental Medicine, Daejeon University, Daejeon, Korea

Available online Mar 12, 2012

Received: Oct 27, 2011
Revised: Jan 18, 2012
Accepted: Jan 27, 2012

KEYWORDS
collagen-induced arthritis;
direct moxibustion;
IGF-1;
myostatin;
phospho-Erk1/2;
skeletal muscle;
TGF-β1

Abstract
In this study, we demonstrate that the direct application of moxibustion significantly enhances muscle regeneration in mice with collagen-induced arthritis (CIA). Twelve Dilute Brown Non-Agouti (DBA)/1 J male mice were randomly divided into the following groups: intact control ($n = 4$), CIA ($n = 4$), and CIA with moxibustion treatment (CIA + moxi, $n = 4$). Mice in the CIA and CIA + moxi groups were immunized twice via intradermal injections of bovine type II collagen (C II) at 3-week intervals. After the second injection, moxibustion was applied to the mouse equivalent of the BL24 and ST36 acupoints with a moxa cone five times/day, every other day (except Sundays), for 3 weeks (a total of 9 treatments were administered). Phospho-Erk1/2, myostatin, TFG-B1, and IGF-1 were analyzed using ELISA. Protein levels in skeletal muscle tissues of the hind limb were analyzed by Western blotting and immunofluorescent staining.

Treatment with direct moxibustion led to a marked improvement in CIA and atrophy of individual muscle fibers. Collagen protein signaling in the muscle of the CIA group was stronger than the control and CIA + moxi groups. Myostatin protein expression, as determined by Western blotting and immunofluorescent staining, were stronger in the CIA group compared with the control and CIA + moxi groups. Immunofluorescent staining confirmed that the CIA group had the strongest TGF-B1 protein signals among the three groups. However, in serum analysis the intact control group showed the strongest TGF-B1 protein signaling. RT-PCR analysis of the muscle tissues of the CIA + moxi group showed significant IGF-1 mRNA expression, and the most intense phospho-Erk1/2 protein signaling was detected in the muscle tissues of the CIA group via Western blotting and immunofluorescent staining. These results confirm that the direct administration of moxibustion at *Shenshu* (BL 23) and *Zusanli* (ST 36) influences muscle regeneration in the CIA mouse model. Our results suggest that the establishment of the moxibustion mechanism will encourage the clinical application of moxi.

☆ This study was supported by the Basic Research Projects of the Ministry of Education, Science, and Technology (grant no. 20110005080).
* Corresponding author. 22-5 Daejeon Oriental Hospital, Dae-heung-Dong, Jung-Gu, Daejeon, Korea.
E-mail: hkeacu@dju.kr

doi:10.1016/j.jams.2012.02.001

1. Introduction

Moxibustion is a traditional oriental medicine that is obtained from the mugwort herb. Moxibustion plays an important role in oriental medical therapies for the treatment and prevention of diseases. During moxibustion therapy, practitioners burn the herb fluff and stick at certain acupuncture points at the lesion sites of the patient. Moxibustion is known for its beneficial effects, specifically pain relief and the restoration of chi flow. Also, it supplies beneficial chi and removes harmful chi by providing warm heat and other pharmacological effects [1,2].

According to a 2007 study, moxibustion therapy is one of the most widely used basic oriental medical techniques in Korea [3]. About 67% of Korean oriental medical doctors have applied this technique for musculoskeletal, digestive, and gynecological diseases. However, the number of studies published on moxibustion is only 7% of all acupuncture studies, based on 2010 statistics [4]. Moreover, most papers were clinical studies or reviews of other research papers [4,5]. Until now, basic experimental studies mostly focused on the effects of moxibustion on immune cells such as B-lymphocytes [6,7], T-lymphocytes [6,7], and NK cells [8]. The clinical application of moxibustion has profound effect on musculoskeletal diseases [5]. However, there is an apparent lack of basic medical studies.

Moxibustion therapy is frequently applied to treat chronic arthritis and musculoskeletal diseases in oriental medical clinics [3,5]. Studies on moxibustion have reported external changes to joints, body weight increases, and decreases in protein levels in arthritis-induced rats [9—11]. However, basic medical studies on moxibustion's direct effects on quality of life are unavailable. Arthritic patients typically suffer from join pain and dysfunction. In addition to these symptoms, arthritis also results in muscle weakness and the complete atrophy of muscles. These factors accelerate declines in activities and the ability to work. Arthritis is a disease that carries a significant threat to quality of life. Along with the increasing age of the population in Organization for Economic Cooperation and Development (OECD) countries, the significance and risk of arthritis are increasing as well. Because of these reasons, further research is required.

In this study, we focused on the effects of the direct application of moxibustion to the *Shenshu* (BL 23) and *Zusanli* (ST 36) acupuncture points in order to determine the regenerative effects of moxibustion on muscles in collagen-induced arthritis (CIA) mouse models, which demonstrate muscle degeneration including decreased muscle content and decreased strength of muscle contractions [12—14]. We analyzed myostatin, TGF-B1, and IGF-1, both histologically and biochemically, as the major indicators of muscle regeneration.

2. Materials and methods

2.1. Experimental animals

All experimental and animal maintenance procedures were performed with approval of the ethics committee on animal experimentation at Daejeon University (Daejeon, Korea). DBA/1 J male mice (6 weeks old; Jackson Laboratory, Bar Harbar, ME, USA) were used in this experiment. All DBA/1 J mice were placed in a room at constant temperature ($25 \pm 1^{\circ}C$) and humidity ($55 \pm 10\%$) and a 12-h light/dark cycle. They were allowed to eat commercial rat chow (no were antibiotics added; Samyang Co., Seoul, Korea) and drink water *ad libitum*. Experiments were commenced at least 1 week after the animals arrived at the laboratory.

2.2. CIA animal model

To induce the CIA mouse model, we measured, separated, and melted bovine type II collagen (2 mg/mL; Chondrex, USA) at 4°C overnight. Freund's complete adjuvant (4 mg/mL; Chondrex, Washington, USA) was added to bovine type II collagen and emulsified. We injected 50 μL of the emulsion into the skin at the base of the tail. Three weeks after the first injection, collagen and Freund's incomplete adjuvant (Chondrex, Washington, USA) were mixed at a 1:1 ratio and injected as just described. Successful induction of CIA was determined via crude observation.

2.3. Experimental groups and treatment

DBA/1 J mice were divided into three different groups ($n = 4$). The groups for our experiments included the non-collagen injection group (intact control group), collagen-injected/ arthritis-induced group (CIA group), and the group that received moxibustion after collagen-injection/ arthritis-induction (CIA + moxi group).

The moxibustion procedure started on the 22nd day after the secondary injection of collagen. All groups of animals were anesthetized using a mixture of ketamine (80 mg/kg) and xylazine (5 mg/kg) before the administration of moxibustion. Kangwha moxibustion was used (Samhwasangjae-buso Company, Kangwha, Korea). Moxibustion (0.025 g) was applied five times to each *Shenshu* (BL 23) and *Zusanli* (ST 36) point on both sides [15]. Moxibustion was ignited by first lighting an incense and then transferring the flame. The treatment was performed three times per week for 3 weeks.

2.4. Enzyme-linked immunosorbent assay

Blood sample were collected from all animals, and the serum was separated by centrifugation. The serum TGF-B level was quantified using the Ready-set-go human/mouse TGF-B1 kit (eBioscience, San Diego, CA, USA). The capture antibody with the coating buffer (100 μL) was placed in a well and incubated overnight at 4°C. After overnight incubation, the plate was washed five times with the wash buffer (1xPBS, 0.05% Tween-20). Nonspecific binding was blocked by incubation with an assay diluent for 1 hour, then washed with the wash buffer. The diluted standard solution and serum samples were loaded into each well, incubated for 2 hours at room temperature, and washed with the wash buffer. The detection antibody was mixed with the assay diluent, loaded into each well, incubated for an additional 1 hour at room temperature, and washed with the wash buffer. The avidin-HRP complex was then added and incubated for 30 minutes. A substrate solution was added and allowed 15 minutes for the color reaction to occur, then the

stop solution (1M H_3PO_4) was added to terminate the reaction. The absorbance was measured by spectroscopy at 450 nm.

2.5. Separation of the muscles and ligament tissue

All animals were sacrificed after 3 weeks of moxibustion treatment. Tibialis muscles and the collateral ligament from the knee of the hind limb were collected. The collected samples were frozen using dry ice and stored in −70°C.

2.6. RNA extraction and reverse-transcription polymerase chain reaction

To observe the expression of mRNA, 1 mL of the easy-BLUE reagent (Intron Biotechnology, Seoul, Korea) was mixed with muscle tissue and solubilized muscle tissue at room temperature. Chloroform (200 μL) was added and centrifuged for 10 minutes at 13,000 rpm. The same amount of 2-propanol was added to 400 μL of the supernatant and incubated for 10 minutes at room temperature. After 5 minutes of centrifugation at 13,000 rpm, 1 mL of 75% ethanol was added to the separated RNA. Then, the separated RNA was centrifuged again for 5 minutes at 10,000 rpm. After removing the ethanol, the sample was added to diethylpyrocarbonate (DEPC) that contained tertiary distilled water and analyzed by spectroscopy at 260 nm. cDNA was synthesized by using 1 μg of oligo-dT and reverse transcriptase (MMLV-RT; Promega, Madison, WI, USA). Polymerase chain reaction (PCR) was performed by using Taq polymerase (Promega, Madison, WI, USA) and specific primers. The PCR conditions were as follow: the initial denaturation procedure was 2 minutes at 94°C, followed by denaturation for 20 seconds at 94°C, annealing for 10 seconds at 55°C, and extension for 1 minute at 72°C. PCR was performed for 30 cycles. The experimental primer for the IGF-1 sequence (forward: CTGGACCAGAGACCC TTTGC; reverse: AGAGCGGGCTGCTTTTGTAG) was then synthesized.

2.7. Immunofluorescent staining

To perform double-immunofluorescent staining, glass slides were washed with ethanol, coated with poly-L-lysine solution (100 μg/mL; Sigma, St. Louis, Missouri, USA) at room temperature, and dried overnight. After freezing the muscle tissues at -20°C, the tissues were sectioned to 20-μm-thick slices. Each section was separately attached to the glass slides. The samples were separated and marked as follows: (i) intact control group, (ii) CIA group, (iii) CIA + moxi group. The tissues were attached to the slides and fixed for 45 minutes in a mixed solution of 4% paraformaldehyde and 4% sucrose in phosphate-buffered saline at room temperature. To avoid nonspecific antigen-antibody reactions, the slides were incubated for 16 hours in a BSA (bovine serum albumin, Sigma, St. Louis, Missouri, USA)-blocking buffer at 4°C. The primary antibodies were diluted in the blocking buffer with 2.5% BSA and 2.5% horse serum, and the sample tissues were incubated for 4 hours at room temperature. After incubation with the primary antibodies, the sections were washed with PBST (PBS plus 0.1% triton X-100). The secondary-antibody solution was prepared by adding fluorescein goat anti-mouse antibody (green; 1:400, Invitrogen, Carlsbad, California, USA) and rhodamine goat anti-rabbit antibody (red; 1:400, Invitrogen, Carlsbad, California, USA) to the blocking buffer that contained 2.5% BSA and 2.5% horse serum. Then, the tissue sections were incubated with the secondary antibody in a dark room for 90 minutes. After incubation with the secondary antibody, the slides were washed three times with PBST. Then, the Hoechst nuclear stain was applied at second washing step, and the samples were washed with PBST, including 0.25% Hoechst 33258 fluorescent dye (Sigma, USA). The sections were observed using a Nikon fluorescent microscope (E-600; Nikon, Japan), and images were captured using a Nikon camera (DXM 1200F; Nikon, Tokyo, Japan). The merged images were produced by using the layer-blending options of Adobe Photoshop (version 7.0). The primary antibodies used in this experiment included monoclonal anti-myostatin (1:400; USBiological, Swampscott, MA, USA), monoclonal anti-TGF-B1 (1:400; ebioscience, San Diego, CA, USA), polyclonal anti-phospho-Erk (1:400; Cell Signaling, Beverly, MA, USA), monoclonal anti-collagen (1:400; Sigma, St. Louis, Missouri, USA), and monoclonal anti-neurofilament 200 (1:400; Sigma, St. Louis, Missouri, USA).

2.8. Western blot analysis

The muscle tissues were washed with ice-cold PBS that included 137 mM NaCl, 10.0 mM Na_2PO_4, 2.0 mM KH_2PO_4 (pH 7.4), and melted with 50—200 μl of triton lysis buffer (20 mM Tris [pH 7.4], 137 mM NaCl, 25.0 mM β-glycerophosphate [pH 7.14], 2.0 mM sodium pyrophosphate, 2.0 mM EDTA, 1.0 mM Na_3VO_4, 1% (v/v) triton X-100, 10% (v/v) glycerol, 5.0 μg/mL leupeptin, 5.0 μg/mL aprotinin, 3.0 μM benzamidine, 0.5 mM DTT, and 1.0 mM PMSF). Then, the protein concentration of each muscle tissues was quantified at 15.0 mg. Proteins (15.0 μg) were resolved in 12% (v/v) SDS polyacrylamide gel (1.5 M Trizma base, 10% g/v sodium dodecyl sulfate, 30% g/v acrylamide, 10% g/v ammonium sulfate, and TEMED) and transferred to Immobilon polyvinylidenedifluoride (PVDF) membranes (Pall Corporation, MI, USA). Each blot was blocked with 3% bovine serum albumin (Sigma, St. Louis, Missouri, USA) blocking buffer in TBST (17 mM KH_2PO_4, 50 mM Na_2HPO_4, 1.5 mM NaCl [pH 7.4], and 0.05% tween-20) for 60 minutes at room temperature, then incubated overnight at 4°C in 0.1% tween-20 in TBS plus 3% bovine serum albumin. The PVDF membranes were incubated with the primary antibodies in the blocking buffer after washing three times with TBST. HRP-conjugated goat anti-rabbit IgG (Santa Cruz Biotechnology, Santa Cruz, CA, USA) or HRP-conjugated goat anti-mouse IgG (Santa Cruz Biotechnology, Santa Cruz, CA, USA) were diluted to 1:2000, dissolved in TBST, and incubated with the membranes for 90 minutes after washing three times. The protein bands on the membranes were detected using the Amersham ECL kit/Western blot detection system (Amersham Pharmacia Biotech, USA). Scientific imaging film (Eastman Kodak Co., Rochester, NY, USA) was used to detect the protein bands. The primary antibodies used in the present study included anti-myostatin (1:2000; USBiological, Swampscott,

Massachusetts, USA), phospho-p44/42 Erk 1/2 kinase antibody (1:4000; Cell Signaling, Beverly, MA, USA), and anti-actin antibody (1:15,000; MP Biomedicals, Irvine, CA, USA).

2.9. Hematoxylin and eosin staining

Muscle tissues were collected and frozen at -20°C. The muscle tissues were sliced using a cryosection machine (cryostat; Leica Co., Heidelberg, Germany) to 20-μm-thick sections and attached to the slides. The slides were stained with a hematoxylin (Sigma, St. Louis, Missouri, USA) solution for 1 minute, washed with tap water, stained with an eosin (Sigma, St. Louis, Missouri, USA) solution for 30 seconds, and then washed again with the eosin stain. Then, the slides were subjected to series of ethanol (50% → 70% → 95%) and xylene dehydrations for 1 minute. Then, the cover glasses were mounted using the mounting medium (Fisher Scientific co, Kalamazoo, MI) and the samples were observed using a light microscope (Nikon, Tokyo, Japan).

2.10. Microscopic analysis of the tissue samples

The tissue sample slides with the immunofluorescent or hematoxylin and eosin (H&E) stains were analyzed using a Nikon fluorescence microscope and light microscope (Nikon, Tokyo, Japan), and the images were captured using a digital camera (DXM1200F; Nikon, Tokyo, Japan) that was connected to the microscope. The captured images were analyzed using ACT-1 software (Nikon, Tokyo, Japan). The images were merged using the layer-screen mode of the photoshop software program (version 7.0, Adobe Inc., San Jose, CA).

2.11. Statistical analysis

Continuous variables were summarized as the means ± standard deviations. Comparisons of the averages between the experimental groups were analyzed by using the two-sample independent t test or ANOVA test. All statistical analyses were carried out using SPSS 14.0 (SPSS Inc, Chicago, Illinois, USA), and p values < 0.05 were considered statistically significant.

3. Results

3.1. Morphological changes to the skeletal muscle

3.1.1. External changes to the skeletal muscle

The external features of the hind limbs of the intact and DBA mice were compared. The ankles and toes of the animals in the CIA group were significantly swollen. In the animals in the CIA + moxi group, the ankles and toes were more swollen than those of the intact group (Fig. 1A).

3.1.2. Cross-sectional changes in the muscle tissue

Cross-sectional changes in the muscle fibers of the experimental group were analyzed by H&E staining. The muscle fibers of CIA group showed more atrophy compared with other groups (Fig. 1B). The cross-sectional area of intact group was 3940 μm^2 and that of the CIA group was 2190 μm^2. This difference indicates significant changes in terms of the cross-sectional area ($p < 0.05$). On the other hand, the cross-sectional area of the CIA + moxi group was 2890 μm^2, significantly larger than that of the CIA group. The area of the CIA + moxi group was just 70% of that of the intact control group ($p < 0.05$) (Fig. 1C).

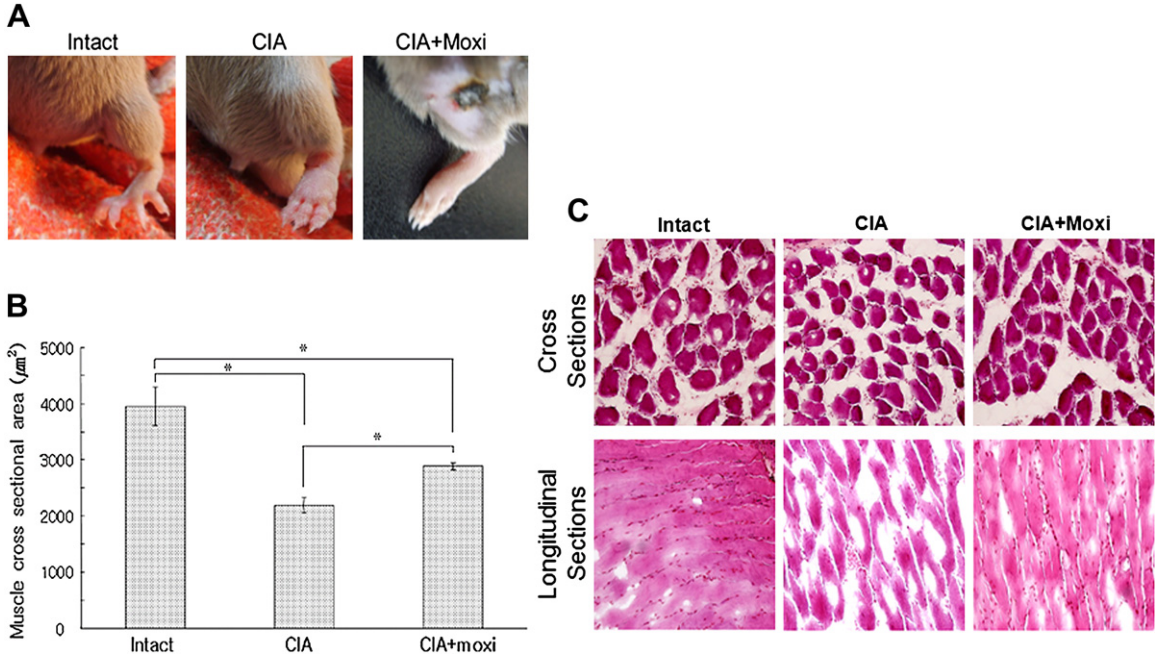

Figure 1 Morphological changes in the skeletal muscle. (A) Photographic images of the hind limb. (B) Quantitative comparisons of muscle size ($n = 3$; error bar = standard error of mean; * $p < 0.05$). (C) Comparison of muscle sections H & E staining.

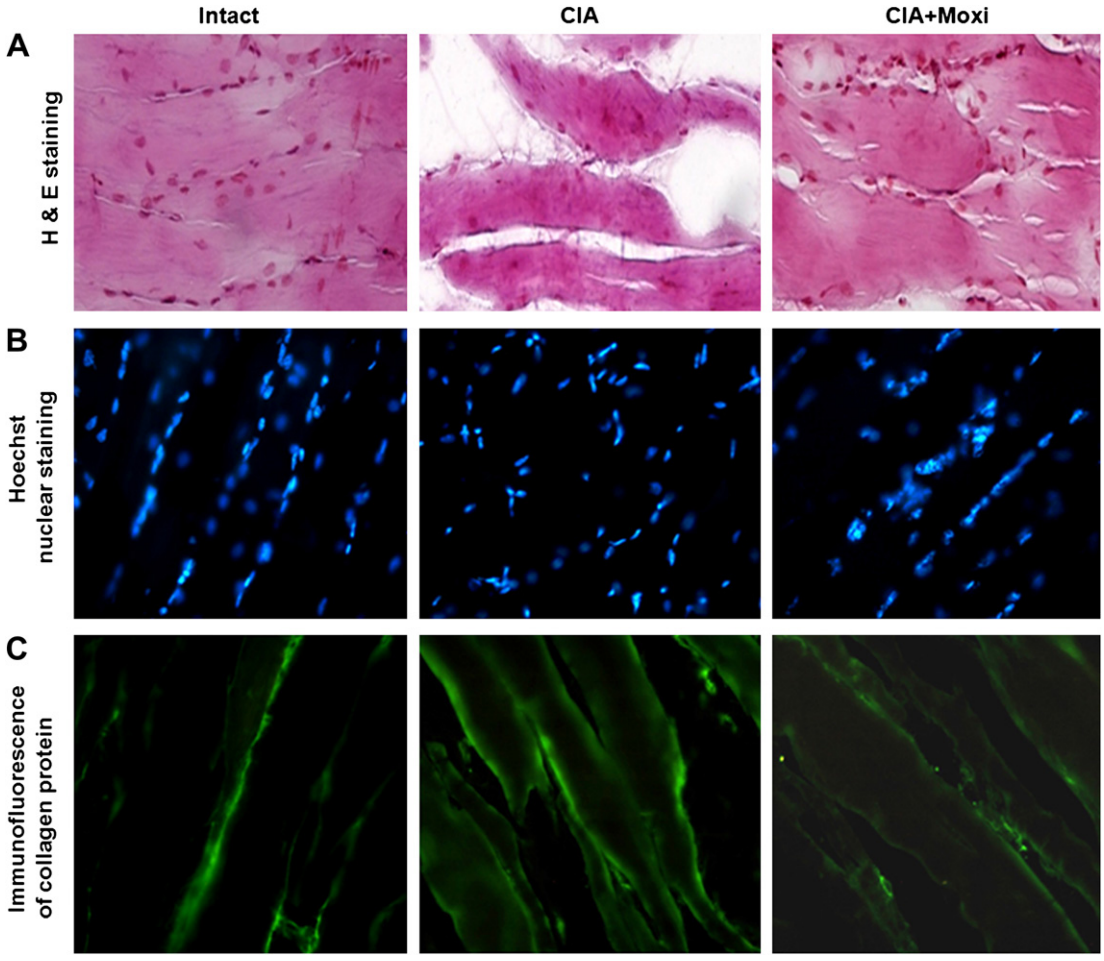

Figure 2 Histological changes in the muscle fibers. (A) Comparison of the cytoplasm by H & E staining. (B) Comparison of the nuclei of individual cells in the muscle tissues by Hoechst 33258 nuclear staining. (C) Immunofluorescent views of collagen protein signals in the muscle tissues.

3.2. Histological changes in the muscle fibers

3.2.1. Comparison of the cytoplasm and nucleus

We compared the H&E staining results of each group's cross-sectional area. The muscle fibers of the intact group showed dense structures without any empty space in the cells. However, several empty spaces in cells, presumably due to atrophy, were observed in the CIA group. Less cellular space and less atrophy were observed in the cells of the CIA + moxi group (Fig. 2A).

Morphological analysis was performed to determine cell viability and cell distribution. This was performed by analyzing high-magnification images of the H&E-stained cells. Hoechst stained-cells demonstrated intact nuclei with linear forms near the muscle cells. The staining intensity in the peripheral regions of the muscle fibers was less intense in the CIA group, whereas the nuclear intensity was higher within the cells. Nuclear staining of the CIA + moxi group showed linear patterns and was similar to that of the intact control group (Fig. 2B).

3.2.2. Level of collagen synthesis

Less-intense collagen staining was observed near the muscle fibers in the intact control group. Collagen staining was prominently higher near the muscle fibers and inside the cells of the CIA group. Overall, collagen synthesis was lower in the CIA + moxi group and showed similar patterns to that observed near the muscle fibers of the intact control group (Fig. 2C).

3.3. Analysis of muscle fiber degeneration and regenerate-related proteins

3.3.1. Analysis of phospho-Erk1/2 protein changes

The phospho-Erk1/2 protein level in the muscle fibers was analyzed using Western blotting. Protein extracts (15 μg) from muscle tissues obtained from the intact, CIA, and CIA + moxi groups (lanes 1—3, respectively) were used for SDS-polyacrylamide gel electrophoresis and further analyzed to detect the phospho-Erk1/2 protein. The same blot was used for actin protein analysis, which was used as an internal loading control. The phospho-Erk1/2 protein level was very high in the intact and CIA groups and relatively low in the CIA + moxi group. The phospho-Erk1/2 protein signal in the intact control group was observed as a long, fibrous shape, and it was observed as a packed, tangled shape in the CIA group. The phospho-Erk1/2 protein signal was only observed in a limited area in the CIA + moxi

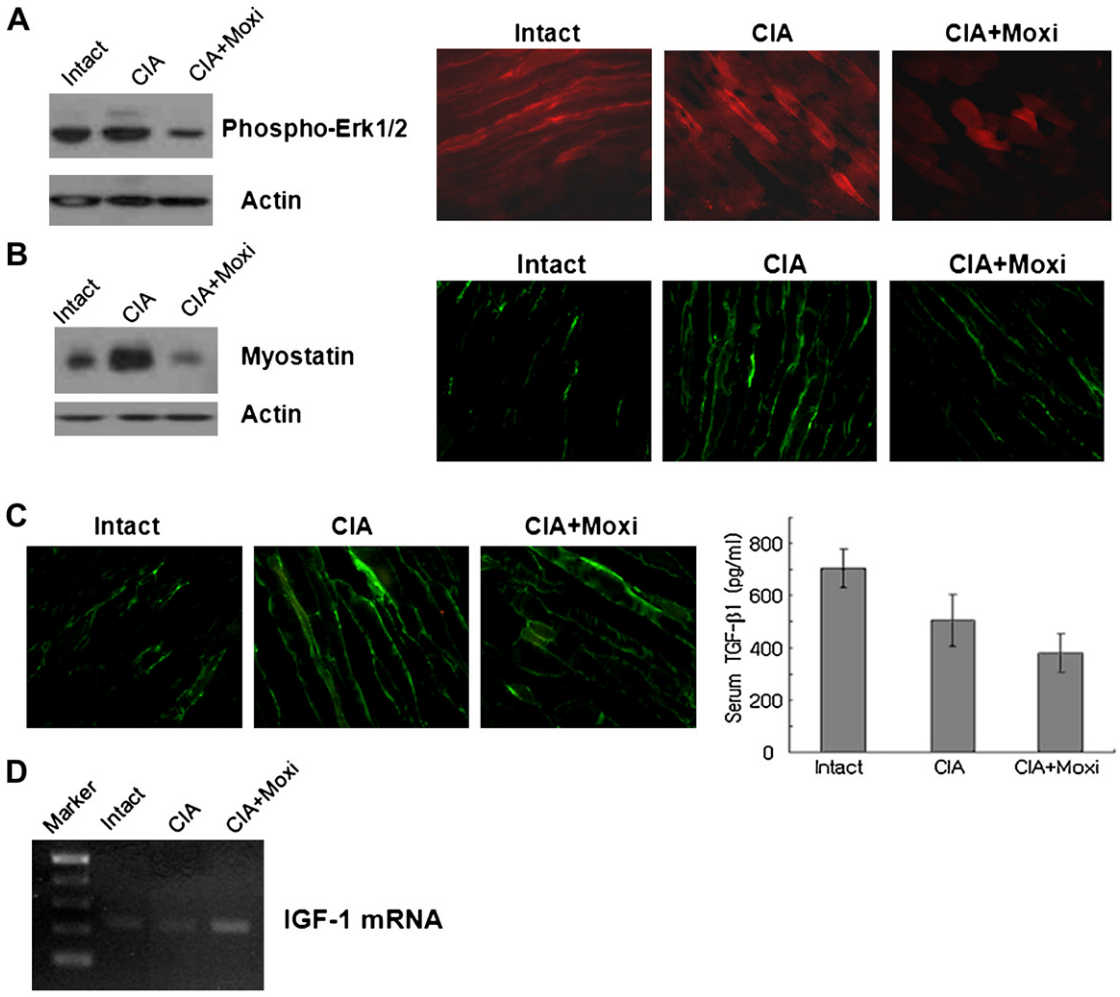

Figure 3 Analysis of muscle fiber degeneration and regeneration-related proteins. (A) Western blot analysis (left) and immunofluorescent views (right) of phospho-Erk1/2 protein signals. (B) Western blot analysis (left) and immunofluorescent views (right) of myostatin protein levels. (C) Immunofluorescent views of TGF-B1 protein signals (left). Measurement of serum TGF-β1 protein levels by ELISA (right). (D) Comparison of IGF-1 mRNA expression levels.

group. This change is consistent with the results of the Western blot analysis of phospho-Erk1/2 (Fig. 3A).

3.3.2. Changes in myostatin protein levels

Western blotting analysis of the myostatin protein demonstrated a consistent myostatin protein level in the intact control group. The CIA group demonstrated the highest level of the myostatin protein, and myostatin protein level in the CIA + moxi group decreased to less than that of the intact control group. In the myostatin immunofluorescent staining results, a prominent linear shape and low protein level were observed. However, a high level of myostatin protein synthesis was observed in the CIA group, and myostatin synthesis decreased in the CIA + moxi group (Fig. 3B).

3.3.3. Changes in TGF-B1 protein levels

The TGF-B1 protein concentration was measured using ELISA. The TGF-B1 protein synthesis levels were decreased in the CIA and CIA + moxi groups compared with that of the intact control group, however these differences were not significant (intact control: 705 ± 75 pg/mL; CIA: 505 ± 99 pg/mL; CIA + moxi: 380 ± 74 pg/mL). On TGF-B1 protein immunofluorescent staining, a low-level, linear, protein signal was observed. On the other hand, in the CIA group, a belt-shaped increase in the TGF-B1 protein level was observed. The protein level in the CIA + moxi group was lower than that of the CIA group, but it was higher than the protein level of the intact control group (Fig. 3C).

3.3.4. Changes in IGF-1 protein levels

Reverse-transcriptase (RT)-PCR was performed to analyze the expression level of IGF-1. Comparisons between amplified DNA and IGF-1 DNA show that the expression of IGF-1 mRNA was higher in the CIA group than the intact control group. In the CIA + moxi group, the IGF-1 mRNA level was higher compared with the other groups (Fig. 3D).

4. Discussion

The therapeutic mechanism of moxibustion lies in the activation of the drug and the generation of warm heat.

Artemisa argyi Lev. Et. Vant. is a herbaceous perennial plant that contains rhizomes, and the leaves are commonly collected and dried during the spring. The leaves contain 0.02% essential oils, the main component of which is cineol that constitutes 50% of the total volume of oils that can be extracted. Other components include, but are not limited to, thujone C13H16O, sesquiterpene, sesquiterpene alcohol, adenine (0.02%), choline (0.11%), and vitamins A, B, C, and D [16]. *A argyi* Lev. Et. Vant. is used in moxibustion, usually to provide consistent, warm heat stimulation that can directly reach deeper parts of the skin and muscle. Hence, *A argyi* Lev. Et. Vant. is used as the main constituent of moxibustion.

The moxibustion procedure was applied at the *Shenshu* (BL 23) and *Zusanli* (ST 36) acupoints of both sides of the hind limbs five times per session, every other day (except Sundays) for 3 weeks (a total of 9 treatments were applied).

Heat stimulated by burning *A argyi* Lev. Et. Vant. is transferred to skin, which is recognized by the thermal sensory receptors as invasive stimulation. This stimulation activates the nerve fibers, which produce the therapeutic effects [17]. The thermal receptors are activated at temperatures above 30°C, and this activation process stops at 49°C. Nociceptors are activated by extreme heat and respond to warm stimulation around 45°C [18]. Generally, the temperature of indirect moxibustion is between 35°—45°C, and about 120—160°C for direct moxibustion [19,20]. Direct moxibustion activates both thermal sensory receptors and nociceptors in the skin. It improves the constitution of the body because of the sterile pyopoiesis that is produced in the local tissues of pustules. Thus, resistive power against diseases increases, helping to treatment and prevention diseases [1].

Moxibustion can also stimulate acupuncture. Moxibustion also has polymodal-afferent, nociceptor-stimulation effects and afferent nerve-stimulation effects, like acupuncture. However, thick afferent nerve fibers (e.g., group 1a and 1b afferent fibers) have lower rates of reactivity to heat, and the effect of moxibustion is lower than that of acupuncture [21]. *Zusanli* (ST 36) is a *shu* acupoint of the stomach channel of the *Foot Yang Ming* meridian and it strengthens the spleen and stomach [22]. The *Zusanli* acupoint is a crucial point that connects eight important acupoints in the lower leg. Stimulating *Zusanli* is known to improve diseases of the leg such as knee joint ache, paralysis or numbness of the lower legs, dermatophytosis of the lower legs, and colic of skin on the knee [23]. *Shenshu* (BL 23) is a *shu* acupoint in the bladder channel of the *Foot Tai Yin* meridian and affects nourishment of the kidney, strengthening of the lumbar vertebrae, and clearing of *suseup* (The pathological substance caused by the malfunction of water metabolism or an excessive water Gi(energy) in the body). Thus, *Shenshu* (BL 23) is clinically used for treating weak kidneys, lumbar pain, spermatorrhea, colic, fatigue, aches of the waist and knees, and small cramps in the knees and feet [22]. The *Zusanli* acupoint has been used in various studies, including electro-acupuncture in arthritis-induced animal models [23] and pharmaco-acupuncture stimulation [24—26]. *Shenshu* (BL 23) has been applied for pharmaco-acupuncture studies on arthritis-induced animal models along with *Zusanli* (ST 36) [26]. *Zusanli* (ST 36) and *Shenshu* (BL 23) are frequently used together in China. It has been reported that *Zusanli* (ST 36) and *Shenshu* (BL 23) have significant effects on most moxibustion applications used to treat arthritis [27—29].

In the present study, moxibustion was applied to a CIA animal model to investigate the effects of direct moxibustion on muscle regeneration-related factors. The results were observed both histologically and serologically. The CIA mouse model resembles diseases such as chronic degenerative arthritis and rheumatoid arthritis in terms of histology, serology, and muscle degeneration. Therefore, the CIA mouse model was suitable for this experiment.

The moxibustion procedure was applied at the *Shenshu* (BL 23) and *Zusanli* (ST 36) acupoints on both side of the hind limbs five times each per session, every other day (except Sundays) for 3 weeks (a total of 9 treatments were applied). The acupuncture points were carefully selected and followed the research guidelines that match mouse acupuncture points and human acupuncture points based on bone locations [15]. We followed previous studies in terms of the amount of moxibustion that was applied [27—29]. However, excess heat stimulation may pose a limitation by inducing traumatic stress factors in the muscle tissues. Since there are no reports on the adequate amount of heat stimulus, efforts were taken to maintain a consistent range of moxibustion stimulation.

Changes and distributions of the collagen protein were analyzed by immunofluorescent staining to investigate changes to the muscle fiber tissue. Due to inflammation caused by tissue damage, fibroblasts in the extracellular matrix were activated. This caused cell proliferation, cell division, and an increase in collagen synthesis. Continued inflammation causes fibrillization [30]. If muscle fiber tissue has regenerative capabilities, fibrilized tissue will be eliminated to a proper level by the action of collagenase in the chronic inflammatory process. Therefore, the collagen protein level after the inflammatory reaction is an indicator of tissue degeneration and is a reflection of regenerative responses. In the present study, collagen was observed near the periphery tissues of the muscle fibers in the intact group. This change might be due to collagen synthesis in the fibroblasts and satellite cells present in the nearby tissues. In addition to the periphery tissues of the muscle fibers, a low level of collagen protein was observed even inside the muscle fibers of the CIA group. The collagen-synthesis level near the periphery muscle tissues was decreased in the CIA + moxi group. The decrease in the collagen protein level was substantial, especially inside muscle fibroblast cells. Therefore, it is hypothesized that these changes are related to the regenerative response of the tissues that were induced moxibustion. This also suggests that moxibustion had an effect on the increase in matrix metalloproteinase (MMP) [31], a breakdown enzyme that disassembles various fibrous proteins in the extracellular matrix such as collagen (Fig. 2C).

The factors involved in the degradation and regeneration of damaged muscle fibers are TGF-B1, myostatin, IGF-1, and others [32,33]. TGF-B1 is an inhibitory factor that differentiates muscle cells and activates muscle fiber formation. TGF-B1 induces activation in the muscle fibroblasts of damaged skeletal muscles. Early muscle fibrillization hinders muscle regeneration and results in the

incomplete recovery of muscles [34]. It is known that treatment with interferon-gamma (IFN-Γ) and suramin facilitates recovery from muscle damage through the inhibition of TGF-B1 activities [35,36]. However, TGF-β1 is common in various organs like the liver, lung, kidney, and heart and is a mediator of fibrillization in various organs. It also plays a role in immunosupressive, anti-inflammatory, and antitumor activities [37—39]. Thus, there is a possibility that the interruption of TGF-B1 synthesis might cause unexpected reactions in the future. On the other hand, myostatin is expressed at a low level in the heart and fat tissues and is expressed at a high level in the skeletal muscles. Previous studies have also shown that myostatin is a better selective target than TGF-B1 for skeletal muscle fibrillization-inhibition therapy [40]. Unlike myostatin and TGF-B1, IGF-1 is a growth hormone that induces the growth of the skeletal muscle cells. IGF-1 also inhibits muscle degeneration, facilitates inflammation, limits fibrillization, and induces the growth of satellite cells. Overall, IGF-1 is involved in all stages of muscle regeneration [41]. There is a report that concludes that minimal expression of IGF-1 in laboratory animals is involved in the muscle atrophy of aging animals [42]. IGF-1 has recently been studied and is believed to be a potential treatment option and an anti-aging substance [43].

The Western blot and immunofluorescent analyses of the myostatin protein described in this study show that the myostatin level was higher in the CIA group than the intact control group. On the other hand, the myostatin level of the CIA + moxi group was similar to that of the intact control group (Fig. 3B). This shows that moxibustion can inhibit myostatin and induce muscle regeneration. The results of the immunofluorescent staining of TGF-B1 also demonstrate that there were no TGF-β1 protein signals in the intact control group. In the CIA group, the TGF-B1 protein signal was prominent in the periphery of the muscle fibers. The TGF-B1 protein signal was lower in the CIA + moxi group compared with the CIA group. However, measurement of the TGF-B1 synthesis level in the serum shows that the TGF-β1 protein level in the CIA and CIA + moxi groups were detected at lower levels compared with that of intact control group, unlike the histological test results (Fig. 3C). It is believed that the difference between the serum and histological tests is due to differences in the systematic and local responses. Because TGF-B1 is synthesized and discharged from various organs, such as the skeletal muscles, heart, lungs, kidneys, etc. [37—39], its level in the serum is systemic. However, histological analysis of the muscle fibers is a measure of the local response in the muscle cells. The results of the serum TGF-B1 protein levels in the CIA and CIA + moxi group suggest that the serum TGF-β1 inhibition mechanism is due to the fact that CIA or moxibustion stimuli act as a stress factor that inhibits various tissues or cell responses. Further research at the cellular level is needed to elucidate how these systematic changes induce regenerative responses in damaged muscle tissue. Also, studies on cell surface-receptor proteins may allow better understanding of the results by analyzing the activities of the receptors.

IGF-1 protein levels were undetectable in serum samples and muscle tissues by Western blot analysis. Thus, we could not directly compare the IGF-1 protein results. Such results may be interpreted as a lack of cross-reactivity between antibodies or insignificant IGF-1 levels. This does not mean, however, that there was no IGF-1 activity. Therefore, we investigated the response of IGF-1 in the muscle tissue to determine the mRNA synthesis level of IGF-1 receptor proteins by RT-PCR. As a result, low-level IGF-1 mRNA expression was confirmed, and the CIA group's mRNA expression was determined to be a little higher than that of the intact control group (Fig. 3D). These results show that moxibustion can activate IGF-1 mRNA expression and contribute to muscle cell regeneration in the muscle tissues of the CIA animals.

This study also investigated the phosphorylated Erk1/2 protein level as one of the other regenerative biological markers responsible for the atrophy of muscle fiber tissue. Erk1/2 is a mitogen-activated protein kinase (MAP kinase) system protein that play a role in cell response to growth stimulation or harmful stimulation [44]. It has been reported that the Erk1/2 protein is synthesized during various stimulations, including stress and growth factors in muscle cells [45—47]. Activation of the Erk1/2 protein promotes the phosphorylation of c-Jun, which is a substrate protein of the JNK protein [48]. And Erk1/2 could activate the apoptosis pathway. The phospho-Erk1/2 protein level was detected at a significantly high level by the Western blot and immunofluorescent analyses. These results suggest that the phospho-Erk1/2 protein might be involved in the activation of muscles, similar to the actin-myosin cross-bridge cycle under normal conditions. Activation of the apoptotic pathway might be related to the increase in phospho-Erk1/2 observed the CIA group, unlike normal muscle. Another possibility includes the activation of phospho-Erk1/2 in atrophic muscles for survival. In the CIA + moxi group, phospho-Erk1/2 was decreased. This is probably the result of heat stimulation and not cell survival-related activities. The histological staining pattern of phospho-Erk1/2 showed that the phospho-Erk1/2 protein signal was observed in both the cell nucleus and cytoplasm. Activation of different substrate proteins in the muscle fiber cell might have different physiological effects.

In conclusion, the direct application of moxibustion at *Senshu* (BL 23) and *Zhusanli* (ST 36) of the CIA animal model contributed to TGF-B1 and myostatin inhibition, IGF-1 activation, and an increase in the nerve fiber distribution. Thus, direct moxibustion at these acupoints seems to have positive effects on muscle regeneration. Based on these results, further research on target cell activation in muscles and satellite cell activation using FoxK1 [49] and Pax-7 [50] is needed. This will further define the mechanisms of muscle regeneration that are affected by moxibustion.

References

1. The Korean Acupuncture & Moxibustion Society; Textbook Compilation Committee. *Acupuncture & Moxibustion Textbook*. 2nd ed. Gyeonggi-do: Jipmundang; 2008.
2. Woo HS, Lee YH, Kim CW. The review and study trend of moxibustion. *J Korean Acupuncture and Moxibustion*. 2002; 19(4):1—15.
3. Han CH, Shin MS, Shin SH, Kang KW, Park SH, Choi SM. Telephone survey for grasping clinical actual state of moxibustion therapeutics in Korea. *Journal of Acupuncture Meridians*. 2007;24(3):17—31.

4. Lee MS, Choi TY, Kang JW, Lee BJ, Ernst E. Moxibustion for treating pain: a systematic review. *Am J Chin Med*. 2010;38(5): 829—838.
5. Park HJ, Son CG. Overview for moxibustion-related researches worldwide. *Journal of Acupuncture Meridians*. 2008;25(3): 167—174.
6. Gil HB, Chung YY. Study on experimental effects of indirect moxibustion on the proliferation of mice lymphocytes. *J Korean Acupuncture and Moxibustion*. 1999;16(4): 271—281.
7. Kung YY, Chen FP, Hwang SJ. The different immunomodulation of indirect moxibustion on normal subjects and patients with systemic lupus erythematosus. *Am J Chin Med*. 2006;34(1): 47—56.
8. Choi GS, Han JB, Park JH, Oh SD, Lee GS, Bae HS, et al. Effects of moxibustion to zusanli on alteration of natural killer cell activity in rats. *Am J Chin Med*. 2004;32(2):303—312.
9. Uryu N, Okada K, Kawakita K. Analgesic effects of indirect moxibustion on an experimental rat model of osteoarthritis in the knee. *Acupunct Med*. 2007;25(4):175—183.
10. Xie XX, Lei QH. Observation on therapeutic effect of the spreading moxibustion on rheumatoid arthritis. *Zhongguo Zhen Jiu*. 2008;28(10):730—732.
11. Kim HK, Kang SK, Park YB. Effects of moxibustion by different methods on blood with adjuvant arthritis in rats. *J Korean Acupuncture and Moxibustion*. 1995;15(2):137—150.
12. Yamada T, Place N, Kosterina N, Ostberg T, Zhang SJ, Grundtman C, et al. Impaired myofibrillar function in the soleus muscle of mice with collagen-induced arthritis. *Arthritis Rheum*. 2009;60(11):3280—3289.
13. Hartog A, Hulsman J, Garssen J. Locomotion and muscle mass measures in a murine model of collagen-induced arthritis. *BMC Musculoskelet Disord*. 2009;3:10—59.
14. Saidenberg-Kermanac'h N, Bessis N, Deleuze V, Bloquel C, Bureau M, Scherman D, et al. Efficacy of interleukin-10 gene electrotransfer into skeletal muscle in mice with collagen-induced arthritis. *J Gene Med*. 2003;5(2):164—171.
15. Yin CS, Jeong HS, Park HJ, Baik YS, Yoon MH, Choi CB, et al. A proposed transpositional acupoint system in a mouse and rat model. *Research in Veterinary Science*. 2008;84:159—165.
16. Lee SI. *Herbal Medicine*. Seoul: Hakrimsa; 1986.
17. Wall, Patrick D, Melzack, Ronald. *Textbook of Pain*. Seoul: Jeongdam; 2002.
18. Guyton AC. *Textbook of Medical Physiology*. Seoul: Jeongdam; 2002.
19. Kim YH, Lee SH, Yeo SJ, Choe IH, Kim YK, Sabina Lim. The study on temperature measurement for the standardization of moxibustion. *J Korean Acupuncture and Moxibustion*. 2008; 25(2):129—138.
20. Yi SH. Thermal properties of direct and indirect moxibustion. *J Acupunct Meridian Stud*. 2009;2(4):273—279.
21. Kenji K, Hisashi S, Kenji I, Fumihiko F, Tadashi Y, Kinya K. How do acupuncture and moxibustion act? *J Pharmacol Sci*. 2006; 100:443—459.
22. The Korean Acupuncture & Moxibustion Society; Textbook Compilation Committee. *Acupuncture & Moxibustion Textbook*. 3rd ed. Gyeonggi-do: Jipmundang; 2008.
23. Hwang HS, Kim EH, Roh JD, Lee EY. Effect of low frequency electroacupuncuture according to acupoint combination on NOS positive neurons in the PAG and hippocampus of rat with adjuvant induced rheumatoid arthritis. *J Korean Acupuncture and Moxibustion*. 2008;25(4):1—9.
24. Kim KS, Yoon JH, Jang JH, Kim KH, Lee SD, Koo MS. The effect of bupleuri radix herbal: acupuncture solution on immune responses to adjuvant induced arthritis in mice. *J Korean Acupuncture and Moxibustion*. 2002;19(3):51—63.
25. Song IK, Choi WS, Park JS, Lee SD, Kim KS. The effect of buthus martensi karsch herbal: acupuncture on immune responses to adjuvant induced arthritis in rats. *J Korean Acupuncture and Moxibustion*. 2002;19(2):177—188.
26. Ryu MS, Yun YC, Kim JH. The effect of Angelica gigas NAKAI pharmacopuncture at ST(36) and BL(23) on Freund's adjuvant arthritis in rats. *J Korean Acupuncture and Moxibustion*. 2010; 27(5):25—34.
27. Wei JL, Liu MX, Lu SF, Qiao XL. The difference of effect on plasma corticosterone content of adjuvant-induced taken off arthritis rats between acupuncture and moxibastion Therapy. *J Chengdu Medical College*. 2008;3(4):283—284.
28. Xie LS, Tang J, Wang L. Effects of moxibustion on the expression of nitricoxide synthase in the hippocampus and dentate gyrus of rheumatoid arthritis rats. *Medical Journal of West China*. 2009;21(5):710—712.
29. Tang J, Xie LS, Wang L. Effects of moxibustion on the expression of nitricoxide synthase in the paraventricular nucleus of hypothalamus of rheumatoid arthritis rats. *Medical Journal of West China*. 2009;21(5):713—715.
30. Myllyharju J, Kivirikko KI. Collagens and collagen-related diseases. *Ann Med*. 2001;33(1):7—21.
31. Vu TH, Werb Z. Matrix metalloproteinases: effectors of development and normal physiology. *Genes Dev*. 2000;14(17): 2123—2133.
32. Kollias HD, McDermott JC. Transforming growth factor-beta and myostatin signaling in skeletal muscle. *J Appl Physiol*. 2008;104(3):579—587.
33. Tomasek JJ, Gabbiani G, Hinz B, Chaponnier C, Brown RA. Myofibroblasts and mechano-regulation of connective tissue remodelling. *Nat Rev Mol Cell Biol*. 2002;3:349—363.
34. Li Y, Foster W, Deasy BM, Chan Y, Prisk V, Tang Y, et al. Transforming growth factor-ß1 induces the differentiation of myogenic cells into fibrotic cells in injured skeletal muscle. *Am J Pathol*. 2004;164:1007—1019.
35. Foster W, Li Y, Usas A, Somogyi G, Huard J. Gammma interferon as an antifibrosis agent in skeletal muscle. *J Orthop Res*. 2003;21:798—804.
36. Chan YS, Li Y, Foster W, Horaguchi T, Somogyi G, Fu FH, et al. Antifibrotic effects of suramin in injured skeletal muscle after laceration. *J Appl Physiol*. 2003;95:771—780.
37. Gressner AM, Weiskirchen R. Modern pathogenetic concepts of liver fibrosis suggest stellate cells and TGF-beta as major players and therapeutic targets. *J Cell Mol Med*. 2006;10:76—99.
38. Gagliardini E, Benigni A. Therapeutic potential of TGF-beta inhibition in chronic renal failure. *Expert Opin Biol Ther*. 2007;7:293—304.
39. Mutsaers SE, Kalomenidis I, Wilson NA, Lee YC. Growth factors in pleural fibrosis. *Curr Opin Pulm Med*. 2006;12:251—258.
40. Li ZB, Kollias HD, Wagner KR. Myostatin directly regulates skeletal muscle fibrosis. *J Biol Chem*. 2008;283:19371—19378.
41. Mourkioti F, Rosenthal N. IGF-1, inflammation and stem cells: interactions during muscle regeneration. *Trends in Immunology*. 2005;26(10):535—542.
42. Barton-Davis ER, Shoturma DI, Musaro A, Rosenthal N, Sweeney HL. Viral mediated expression of insulin-like growth factor I blocks the aging-related loss of skeletal muscle function. *Proc Natl Acad Sci USA*. 1998;95:15603—15607.
43. Scicchitano BM, Rizzuto E, Musarò A. Counteracting muscle wasting in aging and neuromuscular diseases: the critical role of IGF-1. *Aging*. 2009;1(5):451—457.
44. Segal RA, Greenberg ME. Intracellular signaling pathways activated by neurotrophic factors. *Annu Rev Neurosci*. 1996; 19:463—489.
45. Shefer G, Oron U, Irintchev A, Wernig A, Halevy O. Skeletal muscle cell activation by low-energy laser irradiation: a role for the MAPK/ERK pathway. *J Cell Physiol*. 2001;187(1): 73—80.
46. Sonnet C, Lafuste P, Arnold L, Brigitte M, Poron F, Authier FJ, et al. Human macrophages rescue myoblasts and myotubes

from apoptosis through a set of adhesion molecular systems. *J Cell Sci*. 2006;119(12):2497—2507.
47. Yahiaoui L, Gvozdic D, Danialou G, Mack M, Petrof BJ. CC family chemokines directly regulate myoblast responses to skeletal muscle injury. *J Physiol*. 2008;586(16): 3991—4004.
48. Chu C, Alapat D, Wen X, Timo K, Burstein D, Lisanti M, et al. Ectopic expression of murine diphosphoinositol polyphosphate phosphohydrolase 1 attenuates signaling through the ERK1/2 pathway. *Cell Signal*. 2004;16(9):1045—1059.
49. Garry DJ, Yang Q, Bassel-Duby R, Williams RS. Persistent expression of MNF identifies myogenic stem cells in postnatal muscles. *Dev Biol*. 1997;188:280—294.
50. Seale P, Sabourin LA, Girgis-Gabardo A, Mansouri A, Gruss P, Rudnicki MA. Pax7 is required for the specification of myogenic satellite cells. *Cell*. 2000;102:777—786.